

Communication

Facile Synthesis of Two-Dimensional Porous MgCo_2O_4 Nanosheets as Anode for Lithium-Ion Batteries

Fei Wang¹, Yong Liu^{1,*}, Yuanfang Zhao¹, Yue Wang¹, Zhijie Wang², Wanhong Zhang^{1,*}
and Fengzhang Ren^{1,*}

¹ Collaborative Innovation Center of Nonferrous Metals of Henan Province, the Key Laboratory of Henan Province on Nonferrous Metallic Materials Science and Fabrication Technology, School of Materials Science and Engineering, Henan University of Science and Technology, Luoyang 471023, China; 160302290098@stu.haust.edu.cn (F.W.); m18848970515_1@163.com (Y.Z.); 18438616683@163.com (Y.W.)

² Engineering Laboratory for the Next Generation Power and Energy Storage Batteries, Graduate School at Shenzhen, Tsinghua University, Shenzhen 518055, China; wangzjlu@163.com

* Correspondence: liuyong209@haust.edu.cn (Y.L.); zhangwh@haust.edu.cn (W.Z.); renfz@haust.edu.cn (F.R.); Tel.: +86-379-6423-1269 (Y.L. & W.Z. & F.R.)

Received: 31 October 2017; Accepted: 20 December 2017; Published: 24 December 2017

Abstract: Lithium-ion batteries (LIBs) have drawn considerable attention due to their high energy density and good cycling stability. As a transition-metal oxide, MgCo_2O_4 (MCO) is a promising candidate for energy storage applications because of its low-cost and environmental characteristics. Here, MCO porous nanosheets have been successfully synthesized by a microwave-assisted liquid phase method followed by an annealing procedure. As a result, MCO annealed at 600 °C exhibited optimal rate and cycling performances for Lithium storage application. Specifically, when tested as anode materials for Lithium ion batteries, MCO porous nanosheets delivered a high specific capacity of 1173.8 mAh g⁻¹ at 200 mA g⁻¹, and the specific capacity reached 1130.1 mAh g⁻¹ after 100 cycles at 200 mA g⁻¹, achieving 96.3% for the retention rate. The excellent electrochemical performances are mainly attributed to the monolayer porous nanosheet, which provides short transport paths for Li ions and electrons. Results demonstrated that the MCO porous nanosheets are promising electrode materials for Lithium ion batteries applications.

Keywords: MgCo_2O_4 porous nanosheets; microwave assistant liquid phase method; lithium-ion batteries; electrochemical performances

1. Introduction

The demands for advanced rechargeable batteries have multiplied in recent years because of the need to supply electricity to electronic devices that are used in our daily lives. In this context, Lithium-ion batteries (LIBs) have emerged as one of the most widely used energy storage systems for portable electronic devices due to their high energy density and good cycling stability [1–8]. However, the ever-increasing demands for better LIBs require constant innovation, in terms of higher energy density and power density, improved safety, and longer lifespan, especially for electric vehicles (EVs) and smart grids [9–11]. For this expectation, the key to improved LIB performance is in the electrode materials [12,13]. Compared to conventional graphite anodes with limited theoretical specific capacity of 372 mAh g⁻¹, Co_3O_4 with spinel structure has much higher theoretical specific capacity (~890 mAh g⁻¹), and attracts great research attention as anode materials for LIBs [14]. However, due to toxicity and high cost of cobalt, many efforts have attempted to partially replace Co with other eco-friendly and low-cost elements [15,16], such as CuCo_2O_4 [17], FeCo_2O_4 [18,19], ZnCo_2O_4 [20,21], and MgCo_2O_4 [22,23].

Compared to FeCo_2O_4 and NiCo_2O_4 , MgCo_2O_4 (MCO) shows a lower theoretical capacity ($\sim 780 \text{ mAh g}^{-1}$); the inactive MgO , which is formed during the first discharge, could remit volume variations effectively during the following electrochemical reactions, resulting in good cycling stability [23]. Up to now, there have been several reports about MCO as anode materials for LIBs. For instance, Wang et al. [23] synthesized MgCo_2O_4 nanowires on Ni foam via a hydrothermal method followed by annealing treatment. When used as anode materials for LIBs, it could deliver $\sim 940 \text{ mAh g}^{-1}$ at the current density of 2.5 A g^{-1} . Recently, Lee et al. [22] reported multi-shelled MgCo_2O_4 hollow microspheres synthesized by a solvothermal method and subsequent annealing process. Specifically, the MgCo_2O_4 hollow microspheres exhibit high capacity of 1360 mAh g^{-1} at 0.5 A g^{-1} after 100 cycles. Microwave-assisted methods, due to microwave-induced accelerated kinetics, improved the nucleation rate, reduced in the reaction time, and has drawn large attention in the synthesis of oxide materials [24]. To the best of our knowledge, there is still no report on MgCo_2O_4 synthesized by a microwave-assisted method.

In this work, porous two-dimensional MgCo_2O_4 nanosheets were synthesized by a facile microwave-assisted liquid phase method followed by annealing treatments. Through optimizing the annealing temperatures, MCO with a porous nanosheet structure can be attained. The optimal nanostructure can provide cutty transmission routes for Lithium ions and electrons and provide more active sites, resulting in good electrochemical performances. When used as anode materials in LIBs, the MCO with optimal structure exhibits excellent cycling stability and rate capabilities.

2. Materials and Methods

2.1. Synthesis of MgCo_2O_4 Nanosheets

The chemical reagents were of analytical grade and used as received. In a typical synthesis, 1 mmol of $\text{Mg}(\text{NO}_3)_2 \cdot 6\text{H}_2\text{O}$, 2 mmol of $\text{Co}(\text{NO}_3)_2 \cdot 6\text{H}_2\text{O}$, and 12 mmol of $\text{CO}(\text{NH}_2)_2$ were initially dissolved in a solvent that consisted of 210 mL of ethylene glycol (EG) and 30 mL of deionized water to form a transparent solution and then stirred for about 30 min. The attained pink solution was poured into a three-necked flask (500 mL) and fixed in a microwave reactor (SINEO MAS-II, Shanghai China). A continuous microwave heating mode was set up to provide a stable heat source at a microwave power of 700 W. The temperature of the mixed solution quickly rose from room temperature to $140 \text{ }^\circ\text{C}$, and was then maintained at $140 \text{ }^\circ\text{C}$. After refluxed for 30 min, the resulting precipitates were filtered and washed with absolute ethanol and deionized water several times, and then the collected precipitation was dried at $80 \text{ }^\circ\text{C}$ for 12 h. Finally, to attain MgCo_2O_4 nanosheets, the above dried powder was calcinated at 500, 550, 600, and $650 \text{ }^\circ\text{C}$ for 4 h in air with a heating rate of $5 \text{ }^\circ\text{C min}^{-1}$, denoted as MCO-500, MCO-550, MCO-600, and MCO-650, respectively.

2.2. Material Characterization

The crystallographic phase of the as-synthesized samples was characterized by X-ray diffraction (XRD, Bruker D8 ADVANCE, $\text{Cu K}\alpha$ source). And the microstructures and morphology were observed by scanning electron microscopy (SEM, JSM-5610LV, JEOL, Akishima, Japan), and Transmission electron microscopy (TEM, JSM-2100F, 200 kV, Hitachinaka, Naka, Japan) and high-resolution transmission electron microscopy (HRTEM, FEI, TecnaiG2 F30, 200 kV, Hitachinaka, Naka, Japan).

2.3. Electrochemical Measurements

The electrochemical lithium storage performances were evaluated through a two-electrode system. Specifically, high-purity lithium foil ($15.8 \times 0.5 \text{ mm}$) was employed as the counter and reference electrode. To fabricate the working electrode, the slurry was first made by mixing the MgCo_2O_4 samples, Super P carbon and the polyvinylidene fluoride (PVDF) binder at a weight ratio of 70:15:15 in *N*-methyl pyrrolidone (NMP) solvent. After fully stirring, the steady slurry was coated onto conductive copper foil and dried at $80 \text{ }^\circ\text{C}$ for $\sim 12 \text{ h}$. The current collector then punched into a 12 mm-diameter

disk as working electrode, and the active material loading in each disk was weighed to be 0.9 mg to 1.1 mg, corresponding to 0.8–0.97 mg cm⁻². The coin cells (type CR2025) were assembled in an Ar-filled glovebox with low concentrations of water vapor and oxygen (lower than 0.5 ppm). During assembly, the Celgard 2400 was used as separator, while the electrolyte was made of dissolving 1M LiPF₆ into a solvent consisting of ethylene carbonate (EC) and dimethyl carbonate (DMC) (EC/DMC, 1:1 in volume ratio). The galvanostatic charge-discharge performances were evaluated by LAND system (CT2001A, Wuhan, China) between 0.01 and 3.0 V vs. Li/Li⁺. Electrochemical impedance spectroscopy (EIS) was conducted ranging from 100 kHz to 0.01 Hz, and cyclic voltammetry was measured in the range of 0.01–3.0 V (vs. Li/Li⁺) at 0.5 mVs⁻¹, the above two electrochemical testing were carried out on electrochemistry workstation (CHI660C, Shanghai, China).

3. Results and Discussion

3.1. Structure and Morphology

The XRD patterns of MgCo₂O₄ samples synthesized by the microwave-assistant process and subsequent calcination at different temperatures (500, 550, 600, 650 °C) are shown in Figure 1. The diffraction peaks of MgCo₂O₄ calcinated at different temperatures agreed with the standard JCPDS card No. 81-0667 [25]. No other additional phases or impurities can be observed, indicating that MgCo₂O₄ with cubic spinel structures were successfully synthesized. As the calcination temperatures increased, the diffraction peaks become stronger and sharper, which could be clearly observed in the samples calcinated at 500 °C or above, indicating that the crystal size appears larger with the increase in the crystallinity [24].

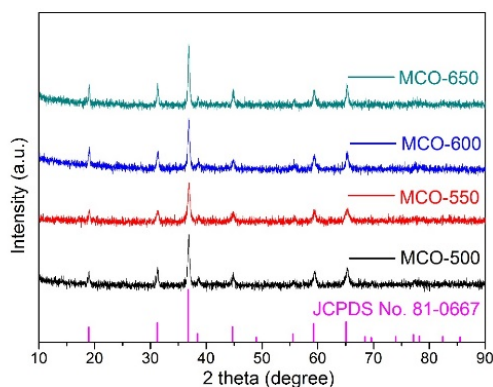


Figure 1. X-ray diffraction (XRD) patterns of MCO-500, MCO-550, MCO-600 and MCO-650.

The SEM images of MgCo₂O₄ samples calcinated at 500, 550, 600, and 650 °C in air for 4 h at a heating rate of 5 °C min⁻¹ are shown in Figure 2. As shown in Figure 2a–c, the as-synthesized MCOs exhibit geometrical sheet-like 2D structures, and the thickness of the nanosheets is about 15–30 nm. Specifically, according to Figure 2a, MCO-500 sample exhibits shaggy and compact nanosheets. When the calcination temperatures increased to 550 and 600 °C, as shown in Figure 2b,c, MgCo₂O₄ samples display unilaminar porous, cross-linked nanosheets with certain dispersity, which could ensure sufficient space between nanosheets for infiltration of electrolyte and buffering volume changes during electrochemical charge–discharge cycling. By contrast, when the calcination temperature continued to increase to 650 °C, there were more macropores on nanosheets; nanosheets changed into nanoparticles, as shown in Figure 2d.

To further explore the microstructure of MgCo₂O₄ nanosheets, TEM, HRTEM, and selected area electron diffraction (SAED) of the MCO-600 sample were carried out, which are shown in Figure 3a–c, respectively. To be specific, as shown in Figure 3a, the TEM image indicates that as-prepared MCO-600 has porous nanosheets morphology with many micropores, and the size of the micropore is 30–150 nm.

The HRTEM image shows regular crystal orientation, as shown in Figure 3b, and the lattice spacing is ~ 0.290 nm, which is corresponding to (220) plane in standard JCPDS card No. 81-0667. Figure 3c shows the SAED image of MCO-600, which indicates that the crystalline structure of as-prepared MCO-600 is spinel structure that is well consistent with the XRD pattern shown in Figure 1.

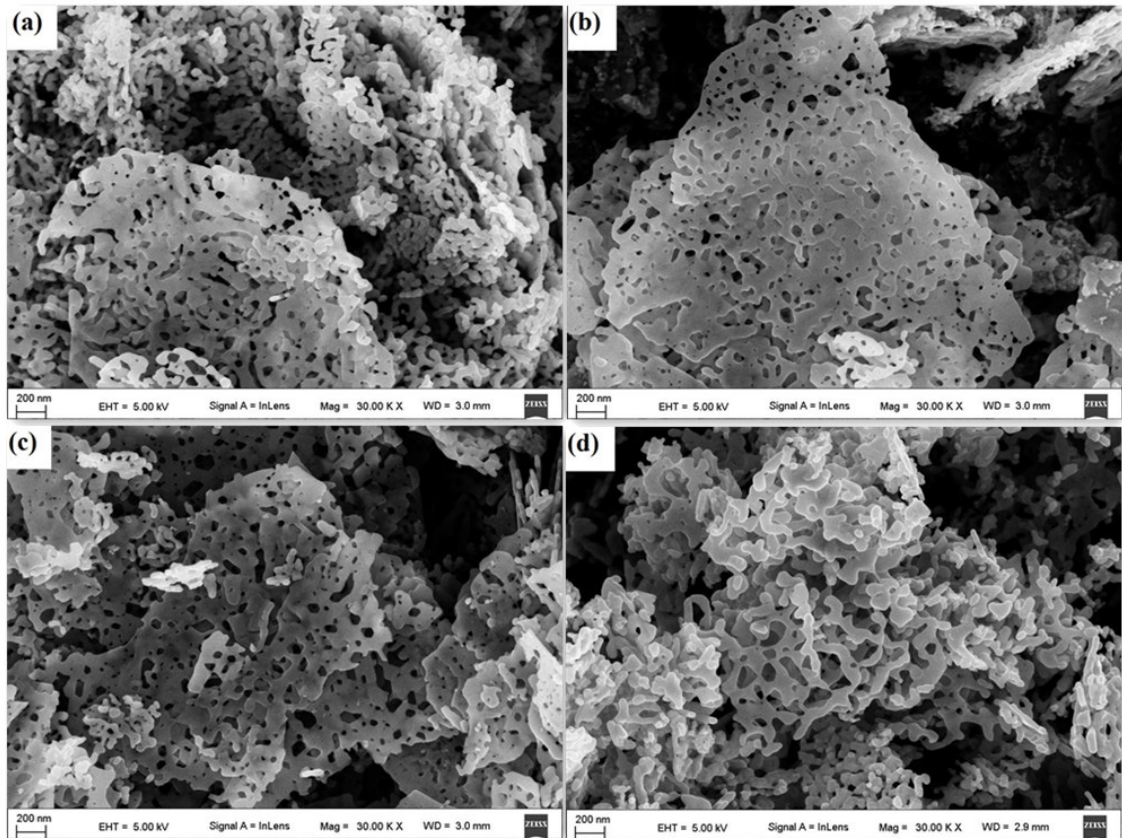


Figure 2. SEM images of (a) MCO-500; (b) MCO-550; (c) MCO-600; (d) MCO-650.

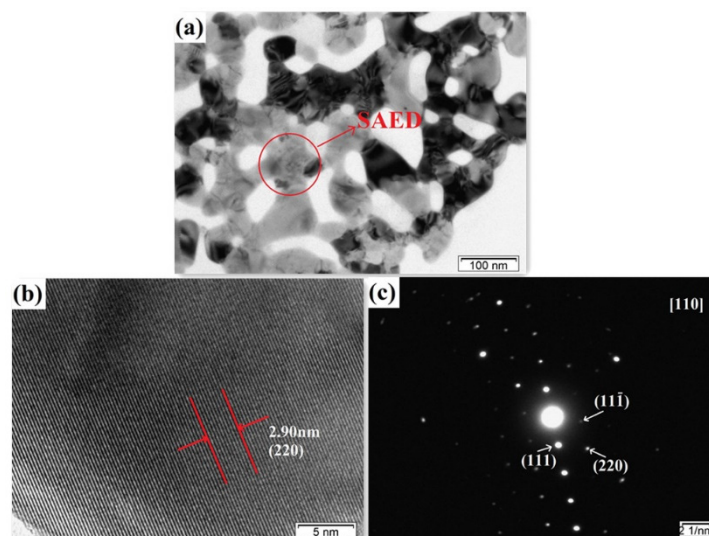


Figure 3. (a) Transmission electron microscope (TEM) image of MCO-600; (b) High resolution transmission electron microscope (HRTEM) image of MCO-600; (c) Selected area electron diffraction (SAED) pattern of MCO-600.

3.2. Electrochemical Properties

The lithium storage properties of MgCo₂O₄ nanosheets at a calcination temperature of 600 °C (MCO-600) was evaluated by cyclic voltammetry (CV) at the scan rate of 0.5 mV s⁻¹ in the voltage range of 0.01–3.0 V, and the first four cycles of CV curves are shown in Figure 4a. The first cathodic peak centered at ~0.75 V could be ascribed to the formation of the solid electrolyte interphase (SEI) layer, which corresponds to the reduction of Co³⁺ to metallic Co⁰ without Mg²⁺ reduction to metallic Mg⁰ because of the strong bond energy in MgO [23]. In the following anodic polarization process, one broad peak centered at around 2.12 V could be ascribed to oxidation of Co to Co²⁺. At the same time, the peak current in the initial cathodic scan is much higher than those in subsequent three cathodic scans, the reason may be that a dramatic reaction comes up when the electrolyte contacts fresh active material in the charge–discharge process, along with fast formation of SEI which is hardly dissolved [26]. In the subsequent three CV cycles, they have similar cathodic peak and anodic peak at ~1.06 V and ~2.16 V, respectively, indicating excellent cycling performance of MgCo₂O₄ [27]. In comparison to the initial CV cycle that has a cathodic peak at 0.75 V and an anodic peak at 2.12 V, the latter three cycles have smaller electrochemical polarization, which indicates that there are better and steady electrochemical kinetics after the initial cycle. On the other hand, the peak area at cathodic scan and anodic scan are similar, which in a certain extent indicates there may be reversible capacity and high coulombic efficiency during charge–discharge cycles. On the basis of the cyclic voltammograms, the entire electrochemical process is classified as follows [22,23]:

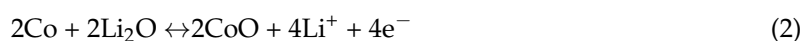


Figure 4b shows the charge and discharge curves of MCO-600 electrode for the first three cycles at the current density of 200 mA g⁻¹. In the first cycle, the specific charge and discharge capacities are about 916.2 mAh g⁻¹ and 1173.8 mAh g⁻¹, respectively. Accordingly, the initial coulombic efficiency is ~78.1%. The charge and discharge capacities are higher than the theoretical capacity of MgCo₂O₄, and extra capacity can be ascribed to SEI formation and the decomposition of electrolyte [23]. In the subsequent cycles, the coulombic efficiency easily reached ~93.3% and 96.6% at the 2nd and 3rd cycles, respectively. Figure 4c gives a comparison of reversible capacity versus cycle number for MgCo₂O₄ annealed at different temperatures (500, 550, 600, and 650 °C). The initial specific discharge capacities of MgCo₂O₄ prepared at 500, 550, 600, and 650 °C, are 983.1, 844.3, 1173.8, and 1030.3 mAh g⁻¹, respectively. As we can see, the specific capacities decrease in the initial cycles, and then increase gradually, which have the same trend as results reported elsewhere [22]. After cycling for 50 cycles, the discharge capacity of MCO-500, MCO-550, MCO-600, and MCO-650 are 1023.4, 720.9, 1254.3, and 990.4 mAh g⁻¹, respectively, and the corresponding capacity retention rates are 104.1%, 85.4%, 106.9%, and 96.1%, respectively. Obviously, as compared to MCO-500, MCO-550, and MCO-650, the MCO-600 shows the highest discharge capacity and superior cycling stability, which may be attributed to the unique porous nanosheet structure of MgCo₂O₄ calcinated at 600 °C. With such an optimal structure, the MCO-600 may not only provide sufficient reaction active sites for Li storage, but also could cope with the volume change during cycling [22].

The rate performances of MgCo₂O₄ calcinated at various temperatures are tested in 0.01–3.0 V at different current densities of 200, 500, 1000, and 200 mA g⁻¹, as shown in Figure 4d. At the current density of 200 mA g⁻¹, the reversible capacity of MCO-600 was 968.5 mAh g⁻¹, while the reversible capacities of MCO-500, MCO-550, and MCO-650 were 921.7, 962.8, and 899.9 mAh g⁻¹, respectively. With the increase of the current density, their reversible capacities were decreased. The MCO-600 anode can still deliver 965.3 and 732 mAh g⁻¹ when the current density increased to 500 and 1000 mA g⁻¹, respectively, which is higher than the anodes prepared from MCO-500, MCO-550,

and MCO-650. For example, the corresponding reversible capacity of MCO-650 anode was 853 and 684.3 mAh g⁻¹. The better rate capability of MCO-600 anode may be attributed to unique nanosheet structure, facilitating fast Li⁺ diffusion and transportation. Figure 4e shows electrochemical impedance spectroscopy (EIS) of MgCo₂O₄ tested ranging from 100 kHz to 0.01 Hz before cycling. The resistance of MCO-600 battery (70.3 Ω) is much smaller than those of MCO-500 (510 Ω), MCO-550 (605 Ω), and MCO-650 batteries (200.1 Ω), which is consistent with the superior cycling performance and cycling capability of MCO-600 anode. When the MCO-600 anode cycled for another 50 cycles, as shown in Figure 4f, the reversible capacity became stable and slightly decreased with the cycle number increased. After 100 cycles, the reversible capacity of MCO-600 was 1130.1 mAh g⁻¹ at a current density of 200 mA g⁻¹, and the corresponding retention rate is ~96.3%, demonstrating good cycling stability of the MCO-600 anode.

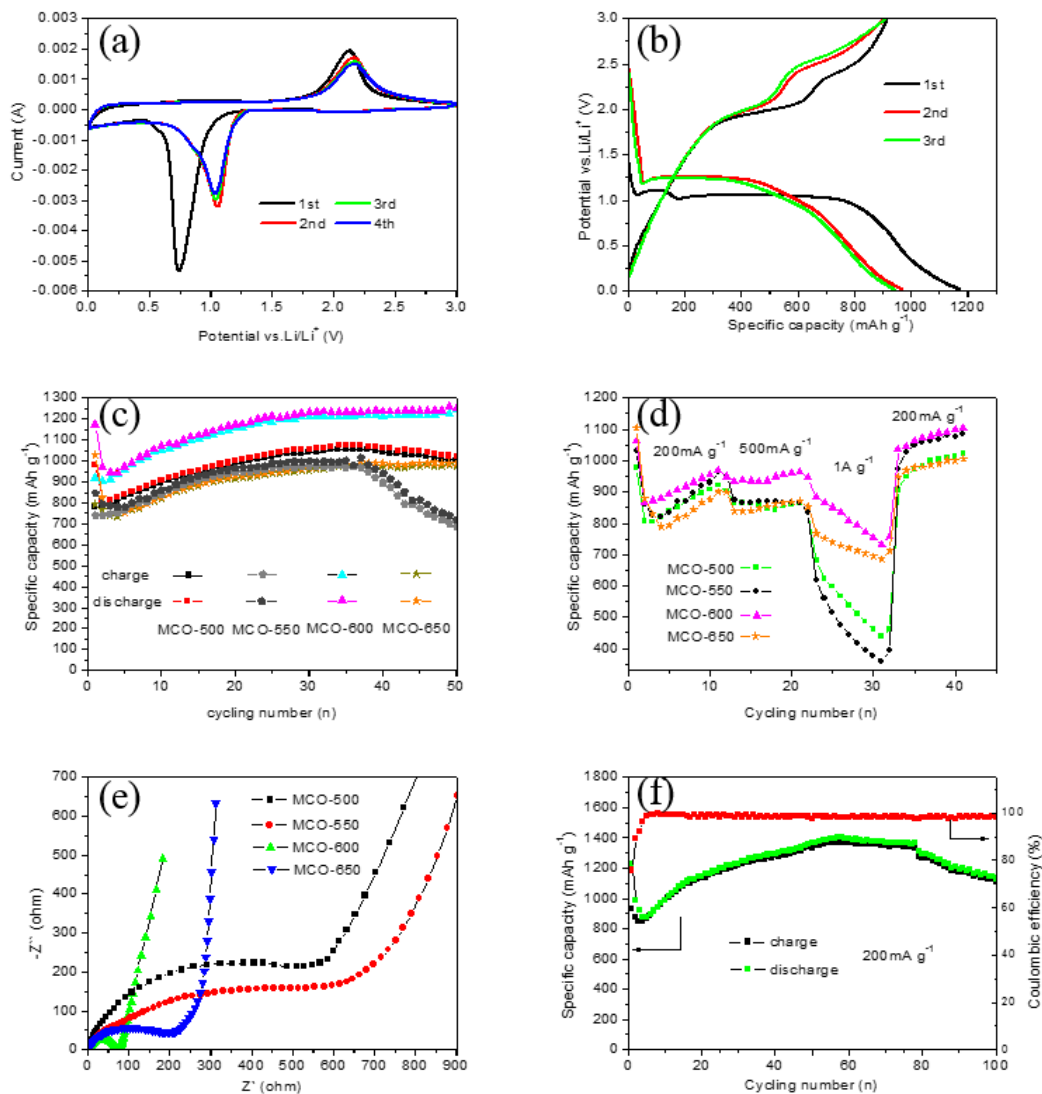


Figure 4. The electrochemical performances of MgCo₂O₄: (a) the initial four CV cycling curves of as-prepared MCO-600 at 0.5 mV/s ranging from 0.01 V to 3.0 V; (b) the initial three galvanostatic charge-discharge curves of MCO-600 at 200 mA g⁻¹; (c) cycling performances of MgCo₂O₄ prepared at various temperatures; (d) rate capability of MgCo₂O₄ prepared at various temperatures; (e) the Nyquist plots of MgCo₂O₄ prepared at various temperatures; (f) long cycling performances of MCO-600 at 200 mA g⁻¹ ranging from 0.01 V to 3.0 V.

4. Conclusions

In summary, MgCo₂O₄ porous nanosheets have been successfully synthesized by a microwave-assisted method and subsequent annealing. According to the comparison of cycling performances and rate capabilities of MgCo₂O₄ calcinated at various temperatures, the MgCo₂O₄ after calcination at 600 °C exhibited good electrochemical performances (with a discharge capacity of 1130.1 mAh g⁻¹ after 100 cycles at a current density of 200 mA g⁻¹). The optimal performance of MCO-600 anode may be attributed to appropriate porous nanosheets structure, which not only provides more active sites for Li ion and electron transportation, but also can cope with the volume expansion of the active materials, demonstrating that the MCO-600 is a promising anode material for Lithium-ion batteries.

Acknowledgments: This study was supported by the Henan International Cooperation Project in Science and Technology (134300510051, 152102410035), the Plan for Scientific Innovation Talent of the Henan Province (144200510009 and 144100510015), the Program for Changjiang Scholars and Innovative Research Team in University (IRT1234), the Program for Science and Technology Innovation Talents in Universities of Henan Province (17HASTIT026) and the Program for Science and Technology Innovation Team of Henan University of Science and Technology (2015XTD006), Scientific Research Starting Foundation for Ph.D. of Henan University of Science and Technology (13480065), and Science Foundation for Youths of Henan University of Science and Technology (2013QN006).

Author Contributions: Yong Liu, Fengzhang Ren, Wanghong Zhang conceived and designed the experiments; Fei Wang, Yuanfang Zhao, Yue Wang performed the experiments; Fei Wang, Yuanfang Zhao, Zhijie Wang and Wanhong Zhang analyzed the data; Fei Wang wrote the paper, Yong Liu revised the paper.

Conflicts of Interest: The authors declare no conflict of interest.

References

1. Tarascon, J.M.; Armand, M. Issues and challenges facing rechargeable lithium batteries. *Nature* **2001**, *414*, 359–367. [[CrossRef](#)] [[PubMed](#)]
2. Armand, M.; Tarascon, J.M. Building better batteries. *Nature* **2008**, *451*, 652–657. [[CrossRef](#)] [[PubMed](#)]
3. Bruce, P.G.; Scrosati, B.; Tarascon, J.M. Nanomaterials for rechargeable lithium batteries. *Angew. Chem. Int. Ed.* **2008**, *47*, 2930–2946. [[CrossRef](#)] [[PubMed](#)]
4. Zhao, Y.L.; Han, C.H.; Yang, J.W.; Su, J.; Xu, X.M.; Li, S.; Xu, L.; Fang, R.P.; Jiang, H.; Zou, X.D.; et al. Stable Alkali Metal Ion Intercalation Compounds as Optimized Metal Oxide Nanowire Cathodes for Lithium Batteries. *Nano Lett.* **2015**, *15*, 2180–2185. [[CrossRef](#)] [[PubMed](#)]
5. Yang, C.; Ou, X.; Xiong, X.; Zheng, F.; Hu, R.; Chen, Y.; Liu, M.; Huang, K. V5S8-graphite hybrid nanosheets as a high rate-capacity and stable anode material for sodium-ion batteries. *Energy Environ. Sci.* **2016**, *10*. [[CrossRef](#)]
6. Ou, X.; Yang, C.; Xiong, X.; Zheng, F.; Pan, Q.; Jin, C.; Liu, M.; Huang, K. A New rGO-Overcoated Sb₂Se₃ Nanorods Anode for Na⁺ Battery: In Situ X-ray Diffraction Study on a Live Sodiation/Desodiation Process. *Adv. Funct. Mater.* **2017**, *27*, 1606242. [[CrossRef](#)]
7. Xiong, X.; Yang, C.; Wang, G.; Lin, Y.; Ou, X.; Wang, J.; Zhao, B.; Liu, M.; Lin, Z.; Huang, K. SnS nanoparticles electrostatically anchored on three-dimensional N-doped graphene as an active and durable anode for sodium-ion batteries. *Energy Environ. Sci.* **2017**, *10*, 1757–1763. [[CrossRef](#)]
8. Zhou, J.; Tao, Q.; Na, X.; Wang, M.; Ni, X.; Liu, X.; Shen, X.; Yan, C. Selenium-Doped Cathodes for Lithium–Organosulfur Batteries with Greatly Improved Volumetric Capacity and Coulombic Efficiency. *Adv. Mater.* **2017**, *29*. [[CrossRef](#)] [[PubMed](#)]
9. Wu, H.B.; Chen, J.S.; Hng, H.H.; Lou, X.W. Nanostructured metal oxide-based materials as advanced anodes for lithium-ion batteries. *Nanoscale* **2012**, *4*, 2526–2542. [[CrossRef](#)] [[PubMed](#)]
10. Zhou, H.S. New energy storage devices for post lithium-ion batteries. *Energy Environ. Sci.* **2013**, *6*, 2256. [[CrossRef](#)]
11. Chang, H.X.; Wu, H.K. Graphene-based nanocomposites: Preparation, functionalization, and energy and environmental applications. *Energy Environ. Sci.* **2013**, *6*, 3483–3507. [[CrossRef](#)]
12. Poizot, P.; Laruelle, S.; Grugnon, S.; Dupont, L.; Tarascon, J.M. Nano-sized transition-metal oxides as negative-electrode materials for lithium-ion batteries. *Nature* **2000**, *407*, 496–499. [[CrossRef](#)] [[PubMed](#)]

13. Zhao, Y.; Li, X.F.; Yan, B.; Xiong, D.B.; Li, D.J.; Lawes, S.; Sun, X.L. Recent Developments and Understanding of Novel Mixed Transition-Metal Oxides as Anodes in Lithium Ion Batteries. *Adv. Energy Mater.* **2016**, *6*. [[CrossRef](#)]
14. Su, X.; Wu, Q.L.; Li, J.C.; Xiao, X.C.; Lott, A.; Lu, W.Q.; Sheldon, B.W.; Wu, J. Silicon-Based Nanomaterials for Lithium-Ion Batteries: A Review. *Adv. Energy Mater.* **2014**, *4*. [[CrossRef](#)]
15. Yuan, C.Z.; Wu, H.B.; Xie, Y.; Lou, X.W. Mixed Transition-Metal Oxides: Design, Synthesis, and Energy-Related Applications. *Angew. Chem.-Int. Ed.* **2014**, *53*, 1488–1504. [[CrossRef](#)] [[PubMed](#)]
16. Sharma, Y.; Sharma, N.; Rao, G.V.S.; Chowdari, B.V.R. Nanophase ZnCo₂O₄ as a high performance anode material for Li-ion batteries. *Adv. Energy Mater.* **2007**, *17*, 2855–2861. [[CrossRef](#)]
17. Pendashteh, A.; Moosavifard, S.E.; Rahmanifar, M.S.; Wang, Y.; El-Kady, M.F.; Kaner, R.B.; Mousavi, M.F. Highly Ordered Mesoporous CuCo₂O₄ Nanowires, a Promising Solution for High-Performance Supercapacitors. *Chem. Mater.* **2015**, *27*, 3919–3926. [[CrossRef](#)]
18. Sharma, Y.; Sharma, N.; Rao, G.V.S.; Chowdari, B.V.R. Studies on spinel cobaltites, FeCo₂O₄ and MgCo₂O₄ as anodes for Li-ion batteries. *Solid State Ion.* **2008**, *179*, 587–597. [[CrossRef](#)]
19. Zhu, H.F.; Sun, Y.F.; Zhang, X.; Tang, L.; Guo, J.X. Evaporation-induced self-assembly synthesis of mesoporous FeCo₂O₄ octahedra with large and fast lithium storage properties. *Mater. Lett.* **2016**, *166*, 1–4. [[CrossRef](#)]
20. Bai, J.; Li, X.G.; Liu, G.Z.; Qian, Y.T.; Xiong, S.L. Unusual Formation of ZnCo₂O₄ 3D Hierarchical Twin Microspheres as a High-Rate and Ultralong-Life Lithium-Ion Battery Anode Material. *Adv. Funct. Mater.* **2014**, *24*, 3012–3020. [[CrossRef](#)]
21. Wu, H.; Lou, Z.; Yang, H.; Shen, G.Z. A flexible spiral-type supercapacitor based on ZnCo₂O₄ nanorod electrodes. *Nanoscale* **2015**, *7*, 1921–1926. [[CrossRef](#)] [[PubMed](#)]
22. Shin, H.; Lee, W.J. Multi-shelled MgCo₂O₄ hollow microspheres as anodes for lithium ion batteries. *J. Mater. Chem. A* **2016**, *4*, 12263–12272. [[CrossRef](#)]
23. Wang, X.J.; Zhai, G.H.; Wang, H. Facile synthesis of MgCo₂O₄ nanowires as binder-free flexible anode materials for high-performance Li-ion batteries. *J. Nanopart. Res.* **2015**, *17*. [[CrossRef](#)]
24. Zhu, Y.; Cao, C.; Zhang, J.; Xu, X. Two-Dimensional Ultrathin ZnCo₂O₄ Nanosheets: General Formation and Lithium Storage Application. *J. Mater. Chem. A* **2015**, *3*, 9556–9564. [[CrossRef](#)]
25. Darbar, D.; Reddy, M.V.; Sundarajan, S.; Pattabiraman, R.; Ramakrishna, S.; Chowdari, B.V.R. Anodic electrochemical performances of MgCo₂O₄ synthesized by oxalate decomposition method and electrospinning technique for Li-ion battery application. *Mater. Res. Bull.* **2016**, *73*, 369–376. [[CrossRef](#)]
26. Mo, Y.; Ru, Q.; Song, X.; Guo, L.; Chen, J.; Hou, X.; Hu, S. The sucrose-assisted NiCo₂O₄@C composites with enhanced lithium-storage properties. *Carbon* **2016**, *109*, 616–623. [[CrossRef](#)]
27. Huang, J.; Fang, G.; Liu, K.; Zhou, J.; Tang, X.; Cai, K.; Liang, S. Controllable synthesis of highly uniform cuboid-shape MOFs and their derivatives for lithium-ion battery and photocatalysis applications. *Chem. Eng. J.* **2017**, *322*, 281–292. [[CrossRef](#)]

